Journal of Biomechanics 45 (2012) 2822–2828

Contents lists available at SciVerse ScienceDirect

Journal of Biomechanics

journal homepage: www.elsevier.com/locate/jbiomech
www.JBiomech.com

Particle-cell dynamics in human blood flow: Implications for vascular-targeted drug delivery

Phapanin Charoenphol [1], Peter J. Onyskiw, Mariana Carrasco-Teja, Omolola Eniola-Adefeso *

Department of Chemical Engineering, University of Michigan, 2300 Hayward Street, 3074 H. H. Dow Building, Ann Arbor, MI 48109, USA

ARTICLE INFO

Article history:
Accepted 30 August 2012

Keywords:
Nanoparticles
Particle dynamics
White blood cells
Endothelial cells
Fluidic chamber

ABSTRACT

The outcome of vascular-targeted therapies is generally determined by how efficiently vascular-targeted carriers localize and adhere to the endothelial wall at the targeted site. This study investigates the impact of leukocytes, platelets and red blood cells on the margination of vascular-targeted polymeric nanospheres and microspheres under various physiological blood flow conditions. We report that red blood cells either promote or hinder particle adhesion to an endothelial wall in a parallel plate flow chamber depending on the blood flow pattern, hematocrit, and particle size. Leukocytes prevent microspheres – but not nanospheres – from adhering in laminar and pulsatile flows via (1) competition for the available binding space and (2) physical removal of previously bound spheres. In recirculating blood flow, the negative effect of leukocytes on particle adhesion is minimal for large microspheres in the disturbed flow region beyond the flow reattachment. Resting platelets were found to have no effect on particle binding likely due to their dimensions and minimal interaction with the endothelial wall. Overall, the findings of the present work would be critical for designing effective vascular-targeted carriers for imaging and drug delivery applications in several human diseases.

1. Introduction

Targeting imaging or drug carriers to endothelium remains attractive for the diagnosis or treatment of several diseases (Bevilacqua et al., 1994; Wickline et al., 2007). In general, vascular-targeted carriers (VTCs) must be designed to successfully (1) navigate the bloodstream while avoiding rapid immune clearance, (2) localize from midstream to the vessel wall in the targeted tissue, and (3) bind at the intended site via specified chemistry. The first attribute has been well investigated (Alexis et al., 2008). The last two attributes constitute carrier margination (localization and adhesion) but have typically only been studied in the context of adhesion via simple flow assays due to the assumption that all particulate carriers can localize to the vascular wall from blood flow (Gentile et al., 2008). To date, few studies have focused on the effects of blood cell dynamics on the margination of VTCs in blood flow to the vascular wall.

In blood flow, red blood cells (RBCs) preferentially move to the centerline thereby forcing leukocytes and platelets to an RBC-free layer (RBC-FL) at the vascular wall (Munn et al., 1996). The high concentration of leukocytes and platelets in the RBC-FL and the RBC ceiling above create a collision dynamic in the RBC-FL that enhances leukocyte and platelet interaction with the wall. This collision dynamic also promotes molecular interaction between cells in the RBC-FL, which further enhances their margination, i.e. secondary recruitment (Walcheck et al., 1996). Since VTCs are often designed to mimic leukocyte margination (e.g. similar adhesive ligands) and must also localize to the RBC-FL to effectively target the vascular wall, it is imperative that the interactions (physical or molecular) between blood cells and VTCs that affect carrier margination be elucidated. Clarity on the nature of these interactions would inform the design of high-performing VTCs. Here, we evaluate the role of blood cells in the margination of sLe^A-coated spheres of various sizes to an inflamed endothelium in human blood flow via *in vitro* flow assays. Laminar flow is explored to represent blood flow in microvessels while pulsatile and recirculating flows typify flow in medium and large arteries. We focus on sLe^A, a carbohydrate that has been previously proposed for targeting the vascular wall (Zhang and Stanimirovic, 2002), due to its favorable binding kinetics with EC-expressed selectins and its involvement in leukocyte–leukocyte secondary recruitment during inflammation response (McEver and Cummings, 1997).

* Corresponding author. Tel.: +1 734 936 0856; fax: +1 734 764 1761.
E-mail address: lolaa@umich.edu (O. Eniola-Adefeso).
[1] Current address: Department of Polymer Science and Engineering, University of Massachusetts-Amherst, Silvio O. Conte National Center for Polymer Research, 120 Governors Drive, Amherst, MA 01003–9263, USA.

0021-9290/$ - see front matter © 2012 Elsevier Ltd. All rights reserved.
http://dx.doi.org/10.1016/j.jbiomech.2012.08.035

2. Methods

2.1. Preparation of endothelial cell (EC)-targeted spheres

Neutravidin–Biotin bonds were used to immobilize sLe^A (Glycotech Corporation) or human ICAM antibody (aICAM) (R&D Systems) onto polystyrene spheres (Bangs; Fishers, IN) (Charoenphol et al., 2010). Ligand density on spheres, characterized via flow cytometry, was fixed at ~1000 sLe^A-site/μm^2 or 5000 aICAM-site/μm^2, unless otherwise stated. These densities are on the order of $sLe^{X/A}$ and β2 integrins densities on human neutrophils, respectively (Latger-Cannard et al., 2003; Rodgers et al., 2000).

2.2. Preparation of EC monolayers

Human ECs harvested from umbilical veins (Mott Children's Hospital, Ann Arbor, MI) were cultured in a tissue culture flask pretreated with 0.2% w/v gelatin (Huang and Eniola-Adefeso, 2012). Endothelial cells were sub-cultured onto circular glass coverslips and kept in a CO_2 incubator until confluent (Eniola-Adefeso et al., 2009). Monolayers were activated with 1 ng/mL IL-1β for 4 or 24 h before use in assays with sLe^A or aICAM-spheres, respectively.

2.3. Preparation of human blood

Fresh blood was obtained via venipuncture as approved by the University of Michigan Internal Review Board with informed consent from subjects. For platelet-depleted blood (PDB), whole blood (WB) was centrifuged to sediment RBCs and leukocytes. Subsequently, platelets were removed from plasma via high-speed centrifugation, and the platelet-poor plasma was recombined with the previously isolated RBC–leukocyte pellets in the original cells-to-plasma ratio. Leukocyte-depleted blood (LDB) was obtained by the addition of 6 wt% dextran to WB to sediment RBCs. The cell-rich plasma was then centrifuged to remove leukocytes only. The leukocyte-depleted plasma was combined with RBCs to achieve LDB. Whole blood with dextran (WB+D) was used as a control for LDB assays. Reconstituted blood (RB; blood devoid of platelets and leukocytes) of a given hematocrit (HCT) was obtained as in Charoenphol et al. (2011).

2.4. Flow adhesion assays

A parallel plate flow chamber (GlycoTech Corporation) with a rectangular straight channel was employed for laminar and pulsatile flow assays as previously described (Charoenphol et al., 2011). Spheres of a given size in blood at 5×10^5 particles/mL were perfused through the flow channel (Fig. 1a) via a syringe pump (KD Scientific). The wall shear rate (WSR) was controlled via blood volumetric flow rate (Eniola-Adefeso et al., 2002). A WSR of 500 s^{-1}, a median of values measured in human microvessels, was employed for laminar flow (Koutsiaris et al., 2007). For pulsatile flow, the pump was run in continuous loops of 14 s of forward flow followed by 7 s of reverse flow for 15 min. This type of pulsatile flow is found in certain regions of large arteries relevant in atherosclerosis (Ku et al., 1985). The same maximum flow rate was used in both directions and set to achieve a WSR of 500 s^{-1} or 1000 s^{-1} for aICAM-1 or sLe^A experiments, respectively. Recirculating flow was generated via a vertical-step flow channel (VSFC; Fig. 1b). A vortex flow is established when laminar flow in the entrance channel expands over the step into the main channel and extends from the step to a reattachment point where flow parallel to the wall is stagnant (i.e. $V_x=0$). Beyond flow reattachment, flow moves forward towards "far downstream" where a laminar flow profile is reestablished. Laminar flow through the VSFC was set to yield a WSR of 200 s^{-1} far downstream. Particle adhesion in the main chamber is observed after 5 min of flow.

2.5. Data analysis

Flow assays were observed at 37 °C on an inverted microscope. Experimental data was recorded and analyzed via Metamorph software. Particle binding per field of view (area=0.152 mm^2, unless otherwise stated) was obtained by manual count. Standard error bars are plotted. Significance in data was analyzed using Student's *t*-test and one-way ANOVA with Tukey post-test. A p value <0.01 was considered statistically significant. The range of particle diameters optimal for adhesion (d_{opt}) for each flow conditions was estimated using a Monte Carlo method where variability in particle size is incorporated with the binding data by sampling sizes within one standard deviation of each average spherical size evaluated (Buckland, 1984). The resulting data sets were subjected to a series of quadratic fits to estimate the d_{opt} range (see Supplementary Appendix A2).

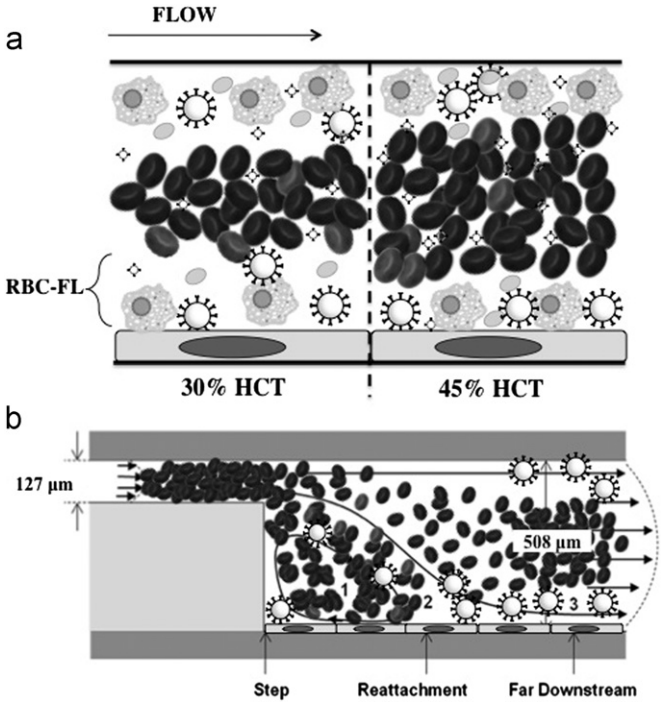

Fig. 1. A schematic representation of blood cell and particle dynamics in the (a) straight and (b) vertical-step flow channel. The enlargement of the RBC core due to higher HCT is shown in (a).

3. Results

3.1. Effect of blood HCT on particle adhesion

For laminar RB flow at 30% HCT, the adhesion of sLe^A spheres increased as the spheres increase in size, from 0.5 to 5.7 μm (Fig. 2a). No significant difference was observed between the adhesion of 0.2 and 0.5 μm spheres. At 45% HCT, the adhesion of 0.5 μm spheres was significantly higher than that of 0.2 μm spheres, and contrary to observation at 30% HCT, 5.7 μm spheres showed adhesion density similar to 2 μm spheres. No adhesion occurred for 10 μm spheres for both HCTs likely due to insufficient adhesion ligands. Adhesion was observed for 10 μm spheres at a higher sLe^A density of 2000 sites/μm^2 (Supplementary Fig. A1; Appendix A). Overall, increasing HCT from 30% to 45% did not affect the laminar flow binding of 0.2 μm spheres, while it significantly enhanced the binding of 0.5 and 2 μm spheres by 205% and 23%, respectively. The adhesion of 5.7 μm spheres was hindered by 18% at the higher HCT. Thus, the estimated range of d_{opt} for the 45% HCT flow, 3.8–4.4 μm, was lower than the range estimated for the 30% HCT flow, 5.1–6.0 μm (Supplementary Table A1; Appendix A).

For pulsatile RB flow (Fig. 2b), the trend in particle binding and the d_{opt} range at 30% HCT was similar to the observation for laminar RB flow at 45% HCT. Only 5.7 μm spheres saw a significant change, a 33% reduction, in their adhesion with higher HCT in pulsatile flow. No binding was observed for 10 μm spheres in pulsatile flow. Thus, the d_{opt} range for the 45% HCT was only slightly lower than the range for 30% HCT. For VSFC assays, there was no difference in the adhesion of all spheres in the recirculation zone between the two HCTs studied (Fig. 2c). Beyond flow reattachment (~300–1000 μm from the step), only 2 and 5.7 μm spheres saw significant increases in their binding levels with the increase in HCT. A plot of particle adhesion at 700 μm from the step (Fig. 2d), an arbitrarily chosen point within the disturbed flow region beyond flow reattachment, yielded d_{opt} ranges